Alien red oak affects soil organic matter cycling and nutrient availability in low-fertility well-developed soils

Alien red oak affects soil organic matter cycling and nutrient availability in low-fertility well-developed soils

Eleonora Bonifacio[1], Marta Petrillo[1], Fabio Petrella[2], Fulvia Tambone[3], Luisella Celi[1*]

[1]. Università di Torino, DISAFA-Chimica Agraria e Pedologia, via L. da Vinci 44, 10095 Grugliasco, Italy

[2]. IPLA-Istituto Piante da Legno e Ambiente, corso Casale 476, 10132 Torino, Italy

[3]. Ricicla Group – Di.S.A.A. - Università degli Studi di Milano - Via Celoria 2 – 20133 Milano, Italy

*** corresponding author: luisella.celi@unito.it**

Abstract

Background and Aims. Invasive alien species can dramatically change the litter and organic matter (OM) decomposition rate, nutrient cycling and availability, thus threatening the ecosystem functionality. We assessed the effect of red oak (QR) introduction on low fertility well-developed soils, originally covered by *Quercus robur L.* (QC).

Methods. We determined litter and soil OM composition and decomposition rate by combining morphological features with ^{13}C NMR spectroscopy, NaClO oxidation and soil respiration. Total and available nutrients were also determined.

Results. The sites showed different humus forms: Dysmull-Hemimoder in QC and Mor in QR. The Oi horizons had a similar composition, but the higher presence of tannins and alkyl C/O alkyl and aryl/O alkyl C ratios in QR indicated that litter was less degradable. This was confirmed by soil respiration tests, with a higher preservation of the NaClO resistant fraction along the profile, mainly due to selective accumulation of alkyl components. This was accompanied by high retention of phosphorus in the organic horizons and drastic reduction of both total and available P in the mineral horizons. Calcium was strongly affected too.

Conclusions. In these well-developed soils red oak changed organic matter dynamics, reduced P availability and cation biocycling, leading the ecosystem functionality towards a no-return threshold.

Keywords

Biocycling; Phosphorus; Oligonutrients; Fragipan; Forest soils; non-resilient ecosystem; Luvisols

Introduction

In recent years, ecosystem invasion by exotic plant species has become a topic of great concern because of threat to biodiversity and disturbances to the original plant community. This is particularly true when considering biodiversity hotspots or natural parks, where a natural or semi-natural environment is meant to be preserved. In general terms, the invasiveness of alien species depends on the budget between positive and negative feedbacks on the environment (Gomez-

Aparicio et al. 2008; Nijjer et al. 2007). Alien species often outcompete with indigenous ones thanks to a number of mechanisms that are not present in the natural communities they invade, and often disrupt equilibria among native species (Callaway and Aschehoug, 2000). These mechanisms may involve the production of allelopathic compounds with direct impacts on native plants (Grove et al. 2013), on microbial communities (Lankau 2011) or mycorrhiza development (Callaway et al. 2008). Furthermore, alien species often show a more favorable allocation of energy hence a more efficient use of nutrients, light and water resources (Closset-Kopp et al. 2011). As tree species differ in litter quality, use of soil nutrients and retranslocation of elements, marked changes in soil properties are expected upon the introduction of non-native species; in case of ecosystems that have lost their ability to return to the original state upon natural or anthropogenic disturbances (i.e. non-resilient ecosystems), the restoration of natural vegetation may be problematic.

Several exotic trees now form a large part of the forest vegetation in Europe; from black locust (*Robinia pseudoacacia* L.) to *Ailanthus altissima* Mill.; from Douglas fir (*Pseudotsuga menziesii* (Mirb.) Franco) to *Prunus serotina* Ehrh. to red oak (*Quercus rubra* L.). Some of them have been introduced for forestry plantations, because of their fast growth and good commercial characteristics, others for land reclamation or due to their ornamental shape and leaf color. Red oak has been introduced in Europe in the 18^{th}-19^{th} centuries and is now posing serious problems to the original vegetation of the mixed broad-leaved forest areas. In many cases in fact, only remnants of the broad-leaved forests persist because of massive agricultural use and land urbanization. For example, the Po river plain in North Italy, was originally covered by forests of the *Carpinion betuli* alliance (*Quercus*, *Tilia*, *Acer*, *Fraxinus* or *Ulmus*), while nowadays is extensively transformed by human activities. In those cases, the rapid growth and the thick canopy of red oak impede the establishment and growth of seedlings from other oak species, impacting the survival of the remaining nuclei of original forests (Ebone and Terzolo 2009). In North America red oak stands are currently declining probably due to the inability of seedlings to compete with shade-tolerant species or in general to physiological stresses that enhance plant susceptibility to pathogen attacks (e.g. Demchik and Sharpe 2000; Kabrick et al. 2008). In Europe instead, it shows prolific regeneration, independently from canopy shading, particularly in low-fertility soils (Major et al. 2013).

In fertility-poor, non-fertilized soils, the dynamics of organic matter and the subsequent biocycling of elements play a key role in maintaining appropriate soil conditions for plant growth (Jobbagy and Jackson 2001). Biocycling of Ca by beech is enhanced in Ca-deficient serpentine soils (Bonifacio et al. 2013) and mineralization of organic P plays a key role in P availability in apatite-poor sandy soils (Celi et al. 2013). The biochemical composition of litter drives the first stages of degradation; the concentration of N-containing compounds and lignin are of utmost importance (e.g. Wedderburn and Carter 1999) as well as the production of microbial stimulators and inhibitors, such as polyphenols and tannins (Talbot and Finzi 2008). The effects alien species have on litter decomposition are not straightforward. In Lithuania, a comparison between two alien maple species and an indigenous one indicated that the alien species have both the lowest and the highest litter decomposition rate (Janusauskaite and Straigyte 2011). Litter from exotic species may be either N-

richer or N-poorer than that of native plants (Ehrenfeld et al. 2001), thus influencing the N to P ratio in the humus layer and potentially shifting the system from a N- to a P-limited one and vice-versa (Wardle et al, 2004). Variations in litter decomposition rates may also be related to the presence of tannins that can change the C/N ratio in the litter, by slowing down the rate of N cycling through the formation of recalcitrant polyphenol-protein complexes (Talbot and Finzi 2008). Oligonutrient concentration in litter also largely differs among species (e.g. Rozen et al. 2010; Staelens et al. 2011) further adding to the variability in available nutrients caused by changing litter decomposition rate.

The aim of this work was to evaluate the effect of past red oak introduction in a natural park in the Po plain of Northwestern Italy. The area is characterized by highly developed, low-fertility soils and the efforts to favor the re-establishment of indigenous vegetation at the expenses of alien red oak have till now always failed. We hypothesized that red oak has changed soil conditions to such a point that failure of restoring the original mixed oak-hornbeam stands is also linked to fertility conditions. The questions we specifically addressed were: 1) is litter and soil organic matter under red oak qualitatively different from that of native broad-leaved forest? 2) what are the mechanisms explaining the differences (if any) in organic matter dynamics under red oak? 3) does red oak affect nutrient availability?

Materials and Methods

Study area and soil sampling

The study area is located in Northwestern Italy, in La Mandria Regional Park, which ranges in elevation from 250 to 420 m a.s.l. (Figure 1). The park was established in 1978 and covers around 1800 ha that were used as hunting reserve of the Savoy royal family since the 16th till the mid of the 20th century. Before it became a natural park, since 1930s and from then on until 1970s, plantations for wood production using the fast-growing North-America red oak were set up in some areas, destroying the climax mixed broadleaved vegetation. Mean annual rainfall is 976 mm with a minimum in summer (July: 67 mm) and a maximum in spring (May: 128 mm). The mean annual temperature is 12.4°C with a minimum in January around +1°C and a maximum of +23°C during summer (data from Venaria weather station, at the south eastern boundary of the park, 255 m asl, Cagnazzi and Marchisio 1998). The area is of fluvioglacial origin and the study sites are located on the gently undulated surfaces of the oldest Pleistocene terraces (Mindel-Riss). The fluvioglacial sediments originated from the Stura di Lanzo basin and form the so-called La Mandria system, composed of highly weathered gravels of serpentinites, gabbros, prasinites, anphibolites, eclogites, gneiss, quartzites and peridotites covered by a thin silt layer (Servizio Geologico d'Italia 2012). On the oldest terraces soils are well developed, homogeneously distributed Oxyaquic Fragiudalfs (Soil Survey Staff 2014). The soil temperature regime is Mesic.

The oldest terraces of the park were surveyed to evaluate soil characteristics that may affect organic matter decomposition, namely redox conditions, evaluated through depth of fragipan, fragipan consistence and development status, and depth to fluctuating water table. All areas close to the

border of the terrace were discarded due to erosion evidences. During the survey, vegetation was also assessed, by taking into account stand composition and canopy cover in red oak areas. We thus selected two plots: QR (i.e. *Quercus rubra* L.) is a stand where tree cover is entirely formed by red oak with no presence of shrubs and little presence of grass cover, while at QC (i.e. Quercus and Carpinus), the upper tree layer is formed by pedunculate oak (*Quercus robur* L.) and sessile oak (*Quercus petraea* (Mattuschka) Liebl.), hornbean (*Carpinus betulus* L.), European ash (*Fraxinus excelsior* L.), wild cherry (*Prunus avium* L.); in the shrub layer common hazel (*Corylus avellana* L.), common hawthorn (*Crataegus monogyna* Jacq.), wild privet (*Ligustrum vulgare* L.) and dog rose (*Rosa canina* L.) prevail, while in the herb layer acidophilous species such as *Luzula nivea* (L.) Lam. et DC., *Calluna vulgaris* (L.) Hull and *Genista germanica* L. are common.

In the middle of the plot a soil profile was dug and described down to the fluctuating water table (between 75 and 100 cm). Samples were taken from both organic and mineral horizons. Additionally, at each plot, four sites were selected within a radius of 12.5 m from the profile, according to ICP Forests sampling procedures (UN/ECE ICP Forests 2006) and samples of soil horizons were taken from pits to take into account the local variability. Although the additional plots cannot be considered true replicates, they were nonetheless used to evaluate small-scale variability in pedologically homogeneous environments. The sequence of soil horizons was the same in the pits and along the profile. The bulk density of the mineral horizons was measured using the core method (Blake and Hartge 1986), while organic layers were sampled using a frame, whose size varied depending on the thickness of organic horizons to collect approximately the same amounts of organic material at all sites. Coarse fragments were found neither in the profile nor in pits. Humus forms were described in the field according to Zanella et al. (2001) who adapted the French system (Brêthes et al. 1995) to the forests of Northern Italy.

Soil chemical analyses

All samples were dried and sieved at 2 mm before the analyses. The pH was determined potentiometrically in a 1:2.5 or 1:20 soil/deionized water suspension for mineral or organic horizons, respectively (Van Reeuwijk 2002). Soil organic C (TOC) and total N (TN) contents were measured by dry combustion (CE Instruments NA2100, Rodano, Italy). The stocks of organic carbon (kg m^{-2}) were calculated as:

$$TOC_{stock} = \frac{thickness \times BD \times TOC}{10}$$

where thickness (dm) refers to soil horizons, BD is the soil bulk density (kg dm^{-3}) and TOC is in g kg^{-1}.

The total Ca, Mg, K and Fe contents (Ca_T, Mg_T, K_T, Fe_T) were determined after HCl-HNO_3 and HF digestion (Bernas 1968) by atomic absorption spectroscopy (AAS, Perkin Elmer 3030, USA). On organic horizons the acid digestion was carried out on previously ignited samples (350°C) to avoid excessive foaming. Total P (P_T) was obtained by molybdate colorimetry after acid digestion with concentrated H_2SO_4 - $HClO_4$ (Kuo 1996). In mineral horizons the pedogenic iron oxide content (Fe_D) was evaluated by the Na dithionite-citrate-bicarbonate extraction (Mehra and Jackson 1960),

the exchangeable amounts of elements were determined by AAS (Ca_{ex}, Mg_{ex}, K_{ex}, Al_{ex}) after extraction with $BaCl_2$ and the CEC was determined by titration after back-exchange of Ba^{2+} with $MgSO_4$. Bioavailable P (P_{av}) was determined using the Olsen method and quantified by malachite-green as described by Ohno and Zibilske (1991). The particle size distribution was evaluated by the pipette method after removal of organic matter and dispersion of the sample with Na-hexametaphosphate. The analyses were duplicated and are reported as average of the 5 soil samples (4 from pits and 1 from the soil profile). For comparative purposes, all analyses which are normally carried out on mineral horizons only, were also performed on the Oa from the QR site.

Organic matter characterization and dynamics

On the organic horizons and on the A from the QC plot, solid-state ^{13}C nuclear magnetic resonance (^{13}C NMR) spectra were acquired with a Bruker AMX 600 spectrometer (Bruker Biospin GmbH, Rheinstetten, Germany), using a 4-mm CP-MAS probe. The spectra were obtained using inverse-gated decoupling, an acquisition time of 0.5 s, a pulse of 45°, and a relaxation delay of 2 s. The number of scans was 24000. The free induction decays were processed by applying 100 Hz line broadening and baseline correction. The chemical shift scale of CP MAS^{13}C NMR spectra were referred to tetramethylsilane (δ = 0 ppm). The ^{13}C NMR spectra were divided in the following regions: 0–45 ppm (C in straight chain, branched, and cyclic alkanes); 45–60 ppm (C in branched aliphatics, amino acids, and OCH_3 groups); 60–110 ppm (C in carbohydrates and aliphatics containing C bonded to OH); 110–160 ppm (aromatic C); 160–220 ppm (C in carboxyl, amide, and ester groups, C in carbonyl groups) (Celi et al., 1997; Almendros et al., 2000; Kögel-Knabner, 2002; Spaccini et al., 2006). Spectra were elaborated using TOPSPIN 1.3 software (Bruker BioSpin GmbH, Rheinstetten, Germany).

The sensitivity of organic matter to chemical oxidation was assessed by treating the organic horizons and the A horizon of the QC plot following the procedure described by Mikutta et al. (2006). The samples were oxidized three times with 6% NaClO at pH 8, then washed with deionized water until the electrical conductivity was below 40 $\mu S\ cm^{-1}$, oven dried at 40°C and the C and N concentrations were determined by elemental analysis. The NaClO-labile carbon pool was obtained by difference between the initial C concentration and the NaClO-resistant C.

The potential organic matter decomposition rates were measured in laboratory during one month lasting experiment. Soil samples (20-50 g for organic horizons and 200 g for mineral ones) were incubated in the dark in precombusted glass microcosms for 30 days at constant temperature (25°C) and humidity (50% of water holding capacity). Mineral samples with less than 7 $g\ kg^{-1}$ of organic C were not taken into account. The microcosms were capped with rubber septa and the air in the headspace was evacuated and replaced with CO_2-free air. The produced CO_2 was collected by removing a 1 mL aliquot of the headspace gas by a syringe. The CO_2 was sampled every two days for the first 10 days and then once a week for the remaining period. The sampled gas was injected into a gaschromatograph (7890A Agilent, Santa Clara, CA, USA) equipped with a Gerstel Maestro autosampler and a packed column (Sigma Aldrich Porapack T) using He as carrier at 30.00 mL/min

flow. CO_2 was detected and measured with a TCD. Injector, column and detector temperatures were kept at 70, 80, and 350°C, respectively. Organic matter mineralization rates from the studied soil samples were calculated by fitting the observed data to the exponential model: $C=C_0\ (1\text{-}e^{-kt})$ where C is the cumulative C mineralized (g kg^{-1} soil) and t is the time in days. The coefficient C_0 (g kg^{-1} soil) gives estimates of the C mineralization potential and K (d^{-1}) is the rate constant.

The characterization of organic matter was performed only on the samples from the soil profiles. All analyses were triplicated.

Statistical analyses

Differences between the two plots were evaluated through a one-way analysis of variance, splitting the dataset according to soil horizons. Before performing the ANOVA, Levene's test for equality of variances was performed and the data checked for normality using the Shapiro-Wilk test. The only variable that did not meet the assumption of homoscedasticity was the Ca_{ex}/Mg_{ex} ratio that was therefore Ln transformed. The correlation between variables was evaluated using the Pearson's coefficient (two-tailed), after a visual inspection of the data to verify that the dependence relationship was linear. A threshold of 0.05 was always used for significance. Data analyses were performed using SPSS 21.

Results

Soil characteristics

Although belonging to the same soil type, the two profiles differed in the upper horizons (Table 1). At the QC site, only Oi and Oe organic layers were found, while at the QR site humified organic horizons (Oa) were present as well. The upper mineral horizons in QC were still influenced by organic matter (A and AE horizons) and showed a discontinuous biomacrostructure, while in QR the transition between organic and mineral horizons was abrupt and an E horizon was found immediately below the organic layers. As a consequence, the two sites had different humus forms: a patchwork of Dysmull-Hemimoder dominated in QC and Mor in QR. The bottom part of the profiles was instead very similar at the two sites with Bt horizons overlying a fragipan (Btx) which was influenced by a fluctuating water table. At both sites clay accumulation started at about 40-45 cm and the amounts of clay in the Bt horizons were similar (24-28%, Table 1). The ratio between Fe_D and Fe_T indicated that 30-40% of Fe was in the form of pedogenic (hydr)oxides and at both sites the highest proportion occurred in the Bt horizons.

The QC plot had lower TOC concentrations than the QR in all horizons (p always <0.05). The TOC concentration of the Oa horizon of QR was close to the lower limit needed for organic materials and the bulk density (1.05 kg dm^{-3}) was high in agreement with the much lower TOC concentration than that of the other organic horizons (Table 1). Total N concentration in organic horizons was the highest in the Oe horizons in both QC and QR, and then decreased with depth, following the OC trend (Table 1). The TOC/TN ratio was similar at the two plots with the exception of the Oi

horizons (higher in QC, $p<0.001$). The higher TOC concentration in all horizons of the QR plot gave rise to TOC stocks that were more than double compared to the QC site (16.5 vs 6.7 kg m^{-2} calculated at 50 cm depth). The higher stocks in QR were mainly caused by the Oe horizon, which stored 11.3 kg m^{-2}.

The CEC ranged from 5.5 to 18.3 $cmol_c$ kg^{-1} for the mineral horizons (Table 2) and was related to both clay and TOC contents ($R^2=0.993$, $p<0.01$). The base saturation followed the pH trend (Table 1) and both Mg_{ex} and Ca_{ex} increased with depth from AE or E horizons to Btx ones (Table 2). With the exception of the uppermost horizons (A and AE in the QC plot and Oa in QR), exchangeable Mg dominated over Ca in all mineral horizons, and the Ca_{ex}/Mg_{ex} ratio was always significantly lower (p always <0.01) at the QR site (Figure 2A). Both the Ca and the Mg saturation of the exchange complex were extremely low in the Oa of the QR plot if compared with the A horizon of the QC (Figure 3). The depth trend of K saturation was instead similar at the two sites. The total concentrations of Ca and Mg were generally higher at QR than at QC in the upper part of the profile while below 10 cm, the differences were less marked or the concentrations were even lower in QR (Table 2). The depth trend of K_T was more variable and QR contents were generally lower than those of QC, with the exception of the Oa vs A horizons. The ratio between total concentrations of Ca and Mg was higher at QC in the upper part of the profile, showed a maximum in the Oe horizons at both sites, then decreased with depth reaching similar values in the mineral horizons of QC and QR (Figure 2B). The total P contents were as well very high in the organic layers of QR and then sharply decreased, while the trend was smoother at the QC plot where the amounts of total P in mineral horizons were much higher than at QR (p always <0.001, Table 2). Available P was very low, with the exception of the A horizon of the QC site. No relationships were found between total and exchangeable concentrations for Ca, Mg and K, while the available P was very well correlated to the total P amounts ($r=0.987$, $p<0.001$).

Soil organic matter characteristics and dynamics

Solid-state ^{13}C NMR spectra and the relative C distribution in the Oi, Oe, Oa/A horizons of the two profiles are shown in Figure 4 and Table 3. The ^{13}C NMR region between 160 and 220 ppm was dominated by a signal at 172 ppm (carboxyl/amide C). The area was of similar intensity in the Oi of both QC and QR profiles, and increased in the underlying horizons especially in QC. In the aromatic and phenolic region, the Oi horizons showed weak signals at 153 and 144 ppm, more pronounced in QR, which revealed a relatively larger presence of phenolic C and tannins (Preston et al. 1997). A low signal at 133 ppm indicated a scarce presence of non-substituted aromatic rings in both Oi horizons. Higher and broader signals were observed in the aromatic region of the other horizons, although, again, the integration area (110-160 ppm) showed a progressive increase only in QC, while in QR it remained nearly constant along the humus profile.

The most prominent signals occurred in the 45-110 ppm region, which included more than 60% of C in the Oi of both sites. The signal at 73 ppm is associated to the simultaneous resonance of C–2, C–3 and C–5 of pyranoside rings in cellulose and hemicellulose, accompanied by the signals at 88

ppm (C-1), 83 ppm (C-4 in amorphous cellulose) and 65 ppm (C–6). The intense signal at 105 ppm was due to anomeric C, highlighting the presence of crystalline cellulose, but it has been attributed also to non-protonated carbon arising from tannins (Wilson et al., 1988). The integration values in the 45-110 ppm region decreased with depth, from 62-64% to 49% in the Oa/A horizons of both profiles, but the reduction was mostly due to the 60-90 ppm region. A shoulder at 56 ppm attributable to lignin methoxyl C confirmed the low presence of lignin in the Oi horizon of both sites, slightly increasing in the other horizons.

In the 0-45 ppm region the signals at 33, 30 and 21 ppm are most likely attributable to paraffinic C of lipids and waxes. The high peak at 33 ppm may be related to $–CH_2–$ C in long alkyl chains such as cutines and suberines. These signals merged in the QC Oe and A as well as in QR A, but a net increase was evident only in the QR Oa (from 24 to 32%). As a consequence the alkyl/O alkyl ratio increased more markedly from the Oi to the Oa of the QR site compared to QC while the opposite occurred for the aryl/O alkyl ratio and the level of aromaticity.

Consistent with the biochemical composition, the distribution between the NaClO-labile and NaClO-resistant fractions was similar in the Oi of both profiles (Figure 5), corresponding to 21 and 79% of TOC, respectively. However, while in the QC profile the rate of decrease from Oi to A was constant, the QR Oe horizon maintained high concentrations of NaClO-resistant C. As a consequence, the NaClO-resistant C was always >70% of TOC in the O horizons of the QR profile, while it decreased from 80 to 61% along the QC profile, depending on the initial C content and C/N ratio ($r=0.918$ and $r=0.877$, respectively, $p<0.001$). The NaClO labile fraction was about 30% of O-alkyl C in the Oi of the QC profile but increased with depth and in the A horizon it was ~75%; by contrast in the red oak plot the NaClO fraction increased from 37 to 58% of O-alkyl C when passing from Oi to Oa horizons. Only small variations in the C/N ratio between labile and resistant organic matter were visible at both sites (Figure 5), and the values reflected those of the original material ($r=0.998$ and $r=0.987$ for resistant and labile organic matter, respectively, $p<0.001$). Moreover the NaClO-resistant organic matter was systematically C-enriched with respect to the labile pool, except in the Oa horizon under red oak (Figure 5).

Nevertheless the comparable litter composition, soil respiration from Oi samples was always slightly higher in QC than in QR during four weeks of incubation (Figure 6A), leading to a carbon mineralization potential of 3.53 and 3.27% of initial TOC (Table 4). In the hemidecomposed organic horizons, a similar trend in CO_2 production was found at the two plots in the first days but afterwards soil respiration started to decrease in QR while in QC it continued to increase. At the end of the incubation period, the Oe samples from the QR and QC plots emitted 2.5 and 3.0 g CO_2-C kg^{-1} soil, respectively, corresponding to 0.51 and 1.1% of initial TOC (Figure 6B). The trend is further confirmed for the Oa or A horizons where the total amount of CO_2 produced in 28 days was about 0.62 and 0.83 g CO_2-C kg^{-1} soil in QR and QC, respectively (0.27 and 1.0% of initial TOC, Figure 6C). The exponential model well described C mineralization from all horizons, accounting for 97–99% of the variation in C mineralization kinetics. In QR K was higher than in QC, except the Oi, and the QR horizons showed lower C_0 than QC (Table 4).

Discussion

In this work we wanted to evaluate the effects that substituting the indigenous mixed broadleaved vegetation with alien red oak had on low fertility soils, in particular on organic matter cycle and nutrient dynamics.

Some differences between the native forest and red oak plots were already visible through field indicators such as humus forms, with a shift from a patchwork of Hemimoder-Dysmull in QC to a homogeneously distributed Mor in QR. These shifts were attributed to unfavorable ecological and site conditions that constrain biological activity (Bernier, 1996; Zanella et al. 2001; Bonifacio et al. 2011) leading to a slowing-down of litter decomposition under red oak. Several factors may affect litter decomposition, either linked to biochemical quality and anatomical features of plant species or soil and environmental conditions (e.g. Kögel-Knabner 2002). Due to the small distance between the sampling sites we can safely discard climate as a factor of variation. The ^{13}C NMR spectra and the relative C distribution among the different groups pointed to a similar biochemical composition of the plant residues found in the Oi horizons of both sites. This is not surprising, because the two plots are dominated by species belonging to the same genus and growing in a restricted geographical area. The plant residues contained a large amount of labile compounds, mostly represented by saccharidic components, as reported for various *Quercus spp.* (Almendros et al. 2000; Chavez-Vergara et al. 2014). However, soil respiration highlighted that only a small fraction of the labile component was used by the microbial community in the 28-day incubation, with slightly lower values in the QR plot than in QC. The subtle difference in the 153 and 105 ppm signals of the ^{13}C NMR spectra between the two Oi horizons indicated a larger presence of tannins in QR (Almendros et al. 2000). The effect of tannins on microbial activity and C and N cycling in soil is species-dependent (e.g. Schimel et al. 1996; Fierer et al. 2001), and Talbot and Finzi (2008) observed that tannins deriving from red oak decreased soil respiration and nutrient availability more than tannins from other species. This is consistent with the fact that red oak tannins may favor the formation of recalcitrant complexes with proteins, affecting both C and N cycling. As a consequence the availability of N might be strongly reduced, leading to a greater accumulation of total N in the organic layers, in agreement with Berthrong and Finzi (2006) and Northup et al. (1995) who found a positive correlation between soil polyphenol concentrations and the accumulation of organic N in soil.

In addition, the slightly higher aromatic C/O–alkyl C and alkyl C/O–alkyl C ratios observed in the Oi of the QR profile may further account for the slowdown in litter decomposition rate. Aromatic C/O–alkyl and alkyl C/O–alkyl C ratios represent indeed a robust indicator for the degree of litter decomposition (Almendros et al. 2000; Bonanomi et al. 2013; Chavez-Vergara et al. 2014). Although these ratios only slightly differed in the Oi horizons, they may have contributed to drive the diverse evolution to Oe-Oa horizons in the red oak plot compared to the sequence Oe-A in the natural system. Chavez-Vergara et al. (2014) also reported that a slightly higher alkyl C/O–alkyl C ratio found in *Q. castanea* litter than in *Q. deserticola* was associated to a lower decomposition rate.

In our system we observed indeed a high persistence of the NaClO-resistant C fraction in the Oe and Oa horizons under red oak, accompanied by an increase of alkyl C, which can be mainly attributed to the selective enrichment of waxes, cutins, etc. The increase in the alkyl C/O–alkyl C ratio was consequently more pronounced in these horizons, suggesting that the organic material was progressively more resistant to microbial degradation than in QC (von Lützow et al., 2006). Conversely, the aromatic C/O–alkyl C varied more in QC than in QR, as in this latter the reduction of holocellulose was less pronounced and accompanied by constancy in the proportion of the aromatic component.

Due to the accumulation of alkyl and condensed molecules, the respiration kinetics sharply diverged in the Oe and Oa/A horizons of the two plots, thus decreasing respiration rate and total CO_2 production beneath red oak. This is in agreement with Nicolini and Topp (2005) who found that microbial activity and respiration rate in red oak plantations on poorly fertile soils were about twice as low as for coetaneous *Q. petraea* and younger *Q. robur* plantations. However, while this induced much higher C stocks under the latter species compared to red oak, in our case an opposite trend was found with the highest stocks in the upper soil horizons of the red oak stand. The drastic reduction of biodiversity with red oak introduction may contribute to further slowdown of decomposition rate leading to such high C stocks.

The different litter degradation pattern in the QR plot had drastic effects on nutrient cycling. In low fertility soils, biocycling of elements is a primary mechanism in sustaining vegetation and typically induces a high availability of elements that are released from litter decomposition in the surface horizons (Bonifacio et al. 2013). We mentioned already that the lower degradation of organic matter in QR, combined with the formation of protein-tannin complexes, may be the main cause of a higher N retention in the organic layers. As a consequence the TOC/TN ratio found in the Oi in the red oak plot was much lower than what expected from litterfall (C/N= 45, data not shown), due to the reduced release of N during litter decomposition (Talbot and Finzi, 2008). Similarly to N, total P in the top layers of the QR plot was extremely high and the resulting TOC/P_T and the TN/P_T ratios were lower than in QC Oi, apparently indicating no P limitation in the humus layers (Wardle et al., 2004). However, the high content of total P was coupled with a much lower P availability and the deeper mineral horizons were remarkably depleted in both total and available P. This may be caused by a more intense nutrient uplift by the fast growing red oak associated with the higher P resorption found in pure oak stands than in mixed ones (Liu et al. 2001). The amount of total P in QR mineral horizons was hence around 35% less with respect to QC, reaching such low values that they did not allow for any further release of available P, further stressing the low fertility conditions.

The similar total amounts of Ca at QR and QC suggested that plants at the two sites incorporate this nutrient cation in similar amounts, in agreement with the results obtained by Dijkstra et al. (2003) who found that Ca weathering, which is directly correlated to total Ca amounts, was more related to the soil parent material than to plant species. Conversely, the higher total Mg concentrations found at the QR site may confirm that Mg uptake is more related to tree physiology than soil contents

(Bukata and Kyser 2008). The availability of both Ca and Mg, depicted by the percentage of cation saturation on the exchange complex, was however much higher in the original mixed broadleaved plot than under red oak. The depth functions for these elements have the typical shape arising from the active ongoing of both leaching and biocycling in the QC stand, while at QR leaching dominated. This decline resulted in soil acidification and increase in extractable Al^{3+} further compromising soil functionality. The availability of K was instead similar at both sites, probably reflecting the lack of a clear trend also in total contents. This situation is not unusual in soils from Northwestern Italy (Bonifacio et al. 2013; D'Amico et al. 2014) and may be related to both the great variability in K contents of the Alpine rocks that originated the sediments of the study areas and to the specificity in K-fixation of vermiculites and degraded illites.

Depletion of P, Ca and Mg by red oak forests is common and has also been found by Hallet and Hornbeck (1997) for sandy soils in the Northeastern United States and Nicolini and Topp (2005). Our study adds to their results by showing that the lower element availability is caused essentially by a decoupling between total and available forms in the case of Ca and Mg, while, for P, even the total pools were nearly exhausted in the deeper soil horizons, thus making the site strongly P-limited and causing serious threats to the original ecosystem restoration.

Conclusions

The introduction of red oak in the areas of the remnants of mixed broadleaved forests of Northwestern Italy has sharply changed soil characteristics, mainly through a variation in the turnover of organic matter that in turn influences the return of nutrient elements into the soil. The effect was however dependent on the kind of element, with Mg and K being the least affected and Ca and P the most. In well-developed soils, where P is a limiting factor for plant growth and the cation exchange complex has already been depleted by leaching of basic cations, the changes induced by alien red oak may drive the ecosystem towards a no-return threshold for the restoration of the original forests. Thus the strategy of invasive species in using competitive mechanisms to disrupt inherent interactions among long-associated native species, becomes particularly effective in poorly fertile soils, ultimately representing a threat to biodiversity and ecosystem services.

Acknowledgements

We thank the staff of the "La Mandria" natural park, in particular Claudio Masciavé and Giusi Rezza, for their help during field surveys.

References

Almendros G, Dorado J, González-Villa FJ, Blanco MJ, Lankes U (2000) ^{13}C NMR assessment of decomposition patterns during composting of forest and shrub biomass Soil Biol Biochem 32: 793–804

Bernas B (1968) A new method for decomposition and comprehensive analysis of silicates by atomic absorption spectrometry. Anal Chem 40:1682-1686

Bernier N (1996) Altitudinal changes in humus form dynamics in a spruce forest at the montane level. Plant Soil 178: 1-28

Berthrong ST, Finzi AC (2006) Amino acid cycling in three cold-temperate forests of the Northeastern USA. Soil Biol Biochem 38:861–869

Blake GR, Hartge KH (1986) Bulk density. In: Klute A (ed) Methods of Soil Analysis. Part 1, 2nd edn. Agron Monogr 9:363–375

Bonanomi G, Incerti G, Giannino F, Mingo A, Lanzotti V, Mazzoleni S (2013) Litter quality assessed by solid state ^{13}C NMR spectroscopy predicts decay rate better than C/N and Lignin/N ratios. Soil Biol Biochem 56: 40–48

Bonifacio E, Falsone G, Catoni M (2013) Influence of serpentine abundance on the vertical distribution of available elements in soils. Plant Soil 368:493-506

Bonifacio E, Falsone G, Petrillo M (2011) Humus forms, organic matter stocks and carbon fractions in forest soils of Northwestern Italy. Biol Fertil Soil 47:555-566

Brêthes A, Brun JJ, Jabiol B, Ponge JF, Toutain F (1995) Classification of forest humus forms: a French proposal. Ann Sci For 52:535–546

Bukata AR, Kyser TK (2008) Tree-ring elemental concentrations in oak do not necessarily passively record changes in bioavailability. Sci Total Environ 390:275-286

Cagnazzi B, Marchisio C (1998) Atlante climatologico del Piemonte. In: Precipitazioni e Temperature, Collana di Studi Climatologici in Piemonte [CD]. Regione Piemonte—Università di Torino, Torino

Callaway RM, Cipollini D, Barto K, Thelen GC, Hallett SG, Prati D, Stinson K, Klironomos J (2008) Novel weapons: Invasive plant suppresses fungal mutualists in America but not in its native Europe. Ecology 89:1043-1055

Callaway RM, Aschehoug ET (2000) Invasive plants versus their new and old neighbors: a mechanism for exotic invasion. Science 290: 521

Celi L, Schnitzer M, Nègre M (1997) Analysis of carboxyl groups in soil humic acids by a wet chemical method, Fourier Transform Infrared Spectrophotometry, and solution-state carbon-13 Nuclear Magnetic Resonance. A comparative study. Soil Sci 162: 189-197

Celi L, Cerli C, Turner BL, Santoni S, Bonifacio E (2013) Biogeochemical cycling of soil phosphorus during natural revegetation of *Pinus sylvestris* on disused sand quarries in Northwestern Russia. Plant Soil 367:121-134

Chavez-Vergara B, Merino A, Vázquez_marrufo G, García-Oliva F (2014) Organic matter dynamics and microbial activity during decomposition of forest floor under two native neotropical oak species in a temperate deciduous forest in Mexico. Geoderma 235-236: 133-145

Closset-Kopp D, Saguez R, Decocq G (2011) Differential growth patterns and fitness may explain contrasted performances of the invasive *Prunus serotina* in its exotic range. Biol Invasions 13:1341-1355

D'Amico ME, Bonifacio E, Zanini E (2014) Relationships between serpentine soils and vegetation in a xeric inner-Alpine environment. Plant Soil 376:11-128

Demchik MC, Sharpe WE (2000) The effect of soil nutrition, soil acidity and drought on northern red oak (*Quercus rubra* L.) growth and nutrition on Pennsylvania sites with high and low red oak mortality. Forest Ecol Manag 136:199-207.

Dijkstra FA, Van Breemen N, Jongmans AG, Davies GR, Likens GE (2003) Calcium weathering in forested soils and the effect of different tree species. Biogeochemistry 62:253-275

Ebone A, Terzolo PG (2009) Monitoraggio, pianificazione e gestione delle specie alloctone invasive di ambienti forestali. In: Nappi P (ed) Rapporto sullo stato dell'ambiente in Piemonte 2009. ARPA-Piemonte, Torino, pp 265-267

Ehrenfeld JG, Kourtev P, Huang W (2001) Changes in soil functions following invasions of exotic understory plants in deciduous forests. Ecol Appl 11:1287–1300.

Fierer N, Schimel JP, Cates RG, Zou JP (2001) Influence of balsam poplar tannin fractions on carbon and nitrogen dynamics in Alaskan taiga floodplain soils. Soil Biol Biochem 33:1827–1839

Gómez-Aparicio L, Canham CD, Martin PH (2008) Neighborhood models of the effects of the invasive *Acer platanoides* on tree seedling dynamics: Linking impacts on communities and ecosystems. J Ecol 96:78-90

Grove S, Haubensak KA, Parker IM (2013) Direct and indirect effects of allelopathy in the soil legacy of an exotic plant invasion. Plant Ecol 213:1869-1882

Hallet RA, Hornbeck JW (1997) Foliar and soil nutrient relationships in red oak and white pine forests. Can J For Res 27: 1233–1244

Janusauskaite D, Straigyte L (2011) Leaf litter decomposition differences between alien and native maple species. Baltic For 17:189-196

Jobbagy E, Jackson R (2001) The distribution of soil nutrients with depth: Global patterns and the imprint of plants. Biogeochemistry 53:51-77

Kabrick JM, Dey DC, Jensen RG, Wallendorf M (2008) The role of environmental factors in oak decline and mortality in the Ozark Highlands. Forest Ecol Manag 255:1409-1417

Kögel-Knabner I (2002) The macromolecular organic composition of plant and microbial residues as input to soil organic matter. Soil Biol Biochem 34: 139–162

Kuo S (1996) Phosphorus. In: Bartels JM, Bigham JM (eds) Methods of soil analysis. Part 3. Chemical methods. SSSA Book Series N° 5. Soil Science Society of America, Madison, pp 869–919

Lankau RA (2011) Intraspecific variation in allelochemistry determines an invasive species' impact on soil microbial communities. Oecologia 165:453-463

Liu CJ, Westman CJ, Ilvesniemi H (2001) Matter and nutrient dynamics of pine (*Pinus tabulaeformis*) and oak (*Quercus variabilis*) litter in North China. Silva Fennica 35:3-13

Lützow M von, Kögel-Knabner I, Ekschmitt K, Matzner E, Guggenberger G, Marschner B, Flessa H (2006) Stabilization of organic matter in temperate soils: mechanisms and their relevance under different soil conditions—a review. Eur J Soil Sci 57 : 426–445

Major KC, Nosko P, Kuehne C, Campbell D, Bauhus J (2013) Regeneration dynamics of non-native northern red oak (*Quercus rubra L.*) populations as influenced by environmental factors: A case study in managed hardwood forests of southwestern Germany. Forest Ecol Manag 291:144-153

Mehra OP, Jackson ML (1960) Iron oxide removal from soils and clays by a dithionite-citrate system buffered with sodium bicarbonate. Clay Clay Miner 9:317–327

Mikutta R, Kleber M, Torn MS, Jahn R (2006) Stabilization of soil organic matter: Association with minerals or chemical recalcitrance? Biogeochemistry 77:25-56

Nicolini F, Topp W (2005) Soil properties in plantations of sessile oak (*Quercus petraea*) and red oak (*Quercus rubra*) in reclaimed lignite open-cast mines of the Rhineland. Geoderma 129:65-72

Nijjer S, Rogers WE, Siemann E (2007) Negative plant-soil feedbacks may limit persistence of an invasive tree due to rapid accumulation of soil pathogens. Proc R Soc B: Biol Sci 274:2621-2627

Northup RR, Yu ZS, Dahlgren RA, Vogt KA (1995) Polyphenol control of nitrogen release from pine litter. Nature 377:227–229

Ohno T, Zibilske LM (1991) Determination of low concentrations of phosphorus in soil extracts using malachite green. Soil Sci Soc Am J 55:892-895

Preston M, Trofymow JA, Sayer BG, Niu J (1997) ^{13}C nuclear magnetic resonance spectroscopy with cross-polarization and magic-angle spinning investigation of the proximate analysis fractions used to assess litter quality in decomposition studies. Can J Bot 75: 1601–1613

Rozen A, Sobczyk T, Liszka K, Weiner J (2010). Soil faunal activity as measured by the bait-lamina test in monocultures of 14 tree species in the Siemianice common-garden experiment, Poland. Appl Soil Ecol 45:160-167

Schimel JP, VanCleve K, Cates RG, Clausen TP, Reichardt PB (1996) Effects of balsam poplar (*Populus balsamifera*) tannins and low molecular weight phenolics on microbial activity in taiga floodplain soil: implications for changes in N cycling during succession. Can J Bot 74:84–90

Servizio Geologico d'Italia (2012) Carta geologica d'Italia 1:50000. Foglio 155 Torino ovest. http://www.isprambiente.gov.it/Media/carg/155_TORINO_OVEST/Foglio.html. Accessed 8 April 2015

Soil Survey Staff (2014) Keys to Soil Taxonomy, 12th ed. USDA-Natural Resources Conservation Service, Washington, DC

Spaccini R, Mbagwu JSC, Conte P, Piccolo A (2006) Changes of humic substances characteristics from forested to cultivated soils in Ethiopia. Geoderma, 132: 9–19

Staelens J, Nachtergale L, De Schrijver A, Vanhellemont M, Wuyts K, Verheyen K (2011) Spatio-temporal litterfall dynamics in a 60-year-old mixed deciduous forest. Ann For Sci 68:89-98

Talbot JM, Finzi AC (2008) Differential effects of sugar maple, red oak, and hemlock tannins on carbon and nitrogen cycling in temperate forest soils. Oecologia 155:583-592

UN/ECE ICP Forests (2006) Manual on Methods and Criteria for Harmonized Sampling, Assessment, Monitoring and Analysis of the Effects of Air Pollution on Forests. 2006 edition. part IIIa on Sampling and Analysis of Soils. Programme co-ordinating centre. http://www.icp-forests.org/pdf/Chapt_3a_2006%281%29.pdf. Accessed 8 April 2015

Van Reeuwijk LP (2002) Procedures for Soil Analysis. Technical Paper n. 9. International Soil Reference and Information Centre, Wageningen

Wardle DA, Walker LR, Bardgett RD (2004) Ecosystem properties and forest decline in contrasting long-term chronosequences. Science 305: 509-513

Wedderburn ME, Carter J (1999) Litter decomposition by four functional tree types for use in silvopastoral systems. Soil Biol Biochem 31:455-461

Wilson MA, Patrick G, Hatcher G (1988) Detection of tannins in modern and fossil barks and in plant residues by high-resolution solid-state ^{13}C nuclear magnetic resonance. Organic Geochemistry 12: 539–546

Zanella A, Tomasi M, De Siena C, Frizzera L, Jabiol B, Nicolini G (2001) Humus Forestali. Manuale di Ecologia per il Riconoscimento e l'Interpretazione. Applicazione alle Faggete. Centro di Ecologia Alpina, Trento

Figure captions

Figure 1 (a) Exchangeable calcium to magnesium ratio and (b) total calcium to magnesium ratio in the soil profiles under *Quercus robur* L. (QC) and *Quercus rubra* L. (QR) in the La Mandria Park.
Figure 2 Exchangeable cation percentage (% of CEC) in the soil profiles under *Quercus robur* L. (QC) and *Quercus rubra* L. (QR) in the La Mandria Park.
Figure 3 Solid state ^{13}C NMR spectra of the top soil horizons under *Quercus robur* L. (QC) and *Quercus rubra* L. (QR) in the La Mandria Park.
Figure 4 NaClO-labile carbon and NaClO-resistant carbon and C/N ratios in the two fractions of the top soil horizons under *Quercus robur* L. (QC) and *Quercus rubra* L. (QR) in the La Mandria Park.
Figure 5 Accumulated CO_2-C production during soil incubation of the top soil horizons (Oi (a); Oe (b) and Oa or A (c)) under *Quercus robur* L. (QC) and *Quercus rubra* L. (QR) in the La Mandria Park.

Figure 1

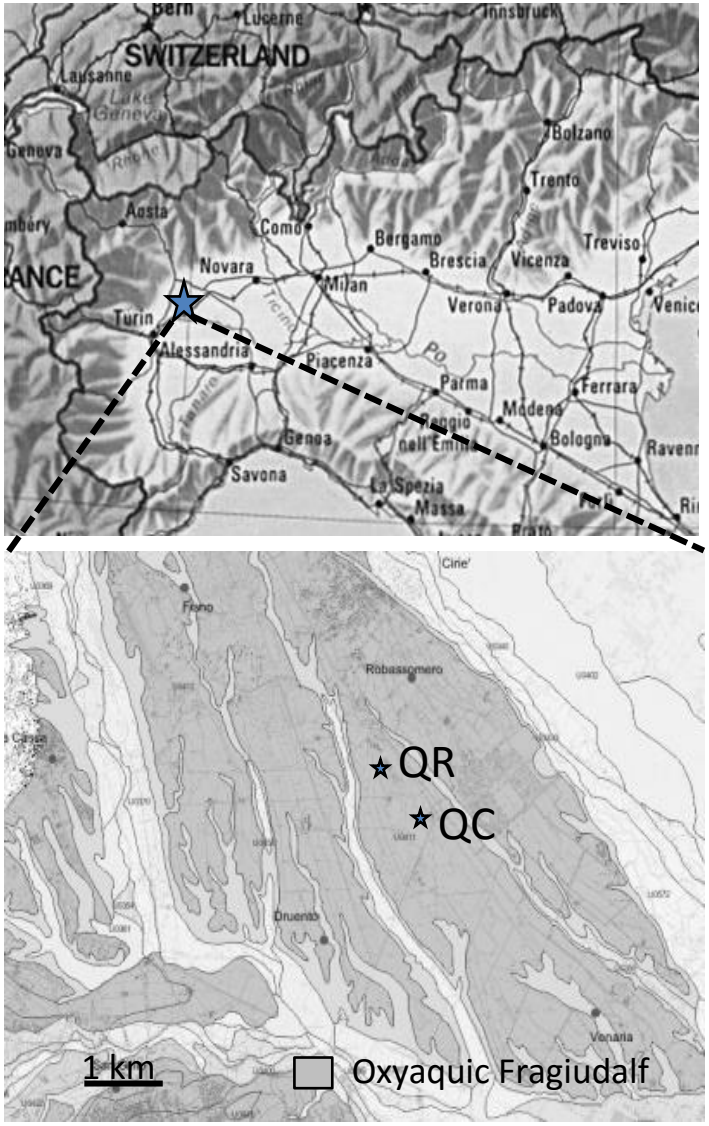
SWITZERLAND
Lausanne
Geneva
Aosta
Como
Bergamo
Brescia
Vicenza
Treviso
Bolzano
Trento
Novara
Milan
Verona
Padova
Turin
Alessandria
Piacenza
Parma
Ferrara
Modena
Bologna
Genoa
Savona
La Spezia
Massa
Cirie'
Fiano
Robassomero
QR
QC
Druento
Venaria
1 km
Oxyaquic Fragiudalf

Figure 1

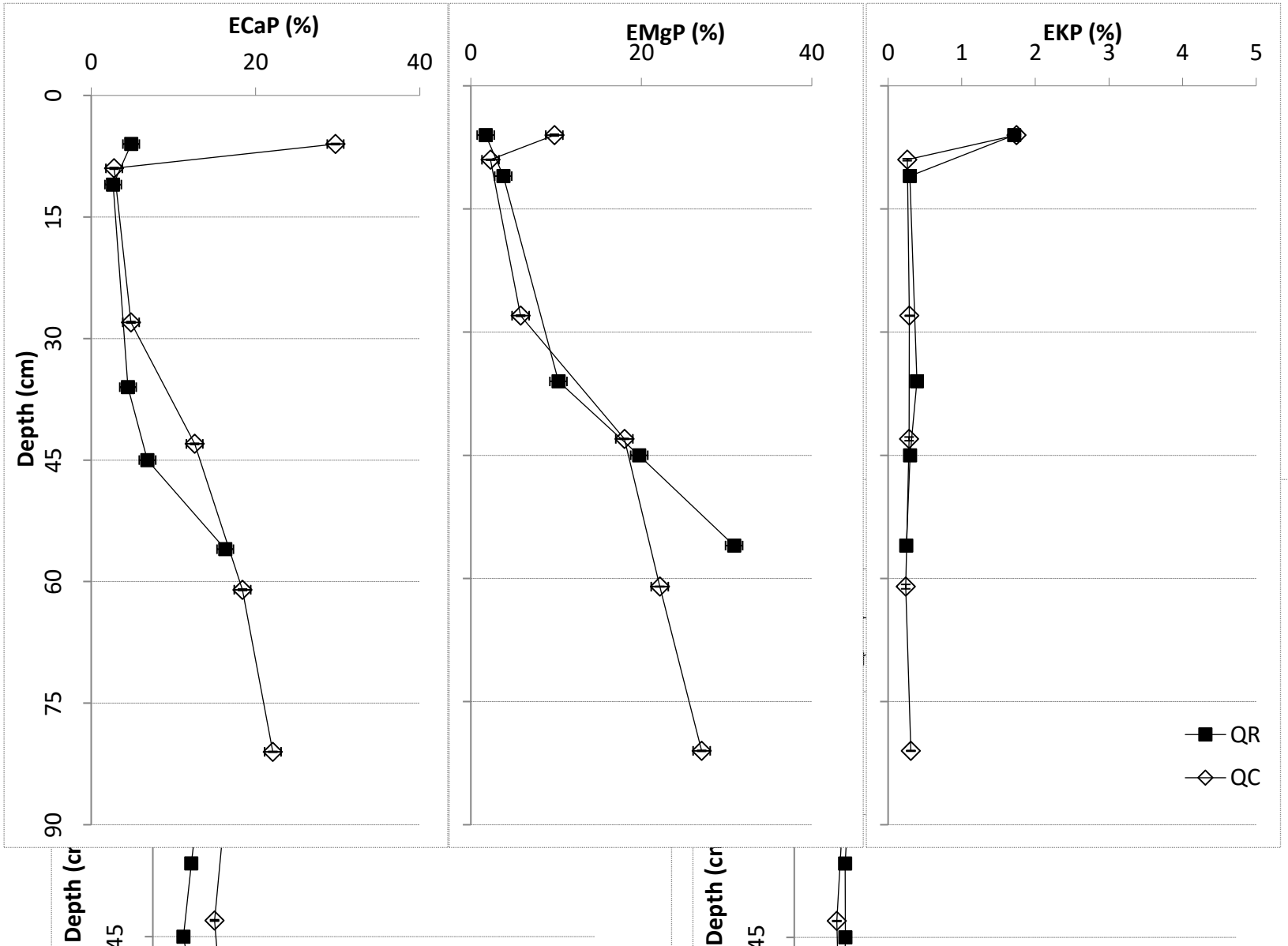

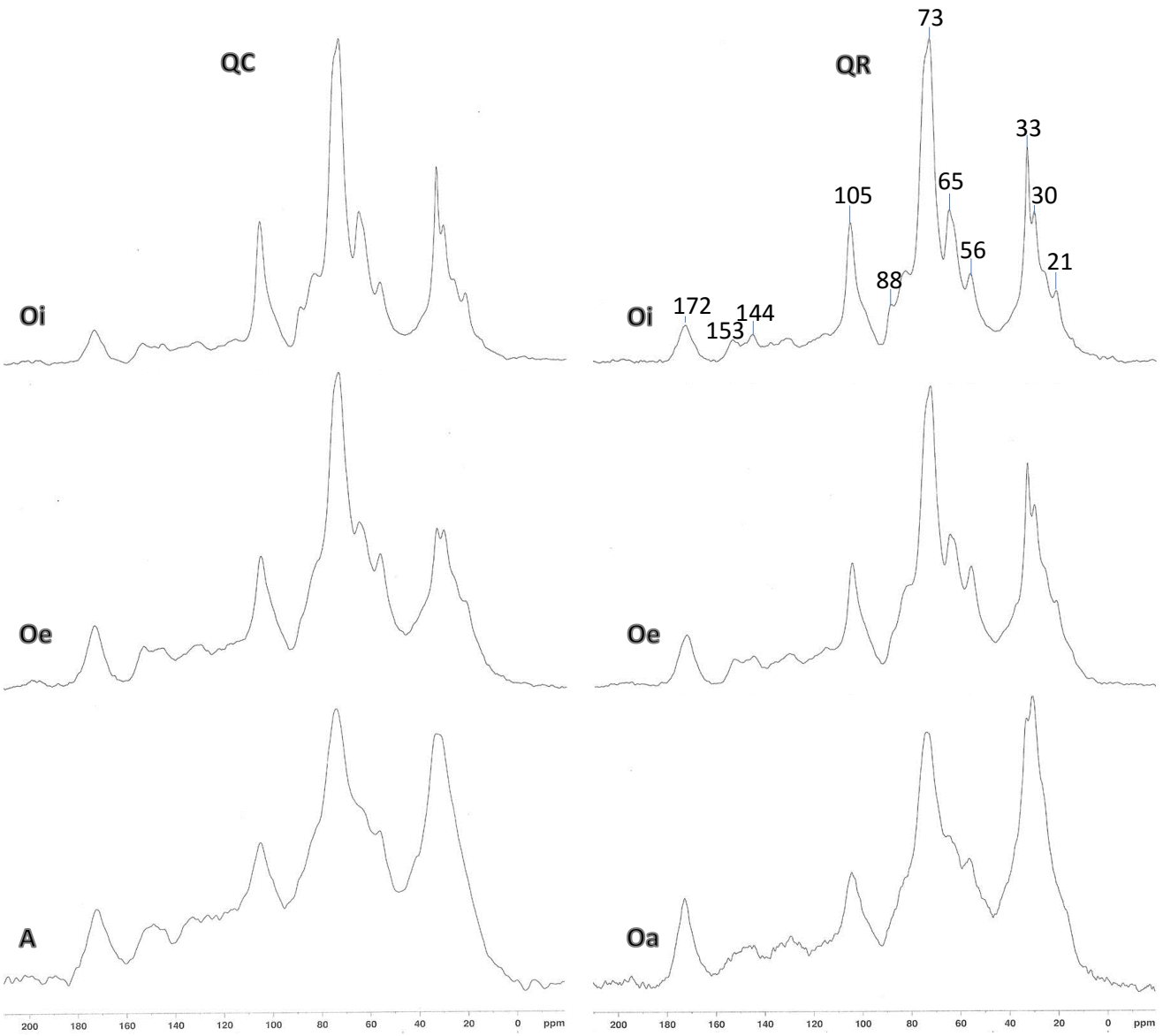
QC
Oi
Oe
A
200
180
160
140
120
100
80
60
40
20
0
ppm
QR
Oi
Oe
Oa
73
33
105
65
30
56
88
21
172
153
144

Figure 3

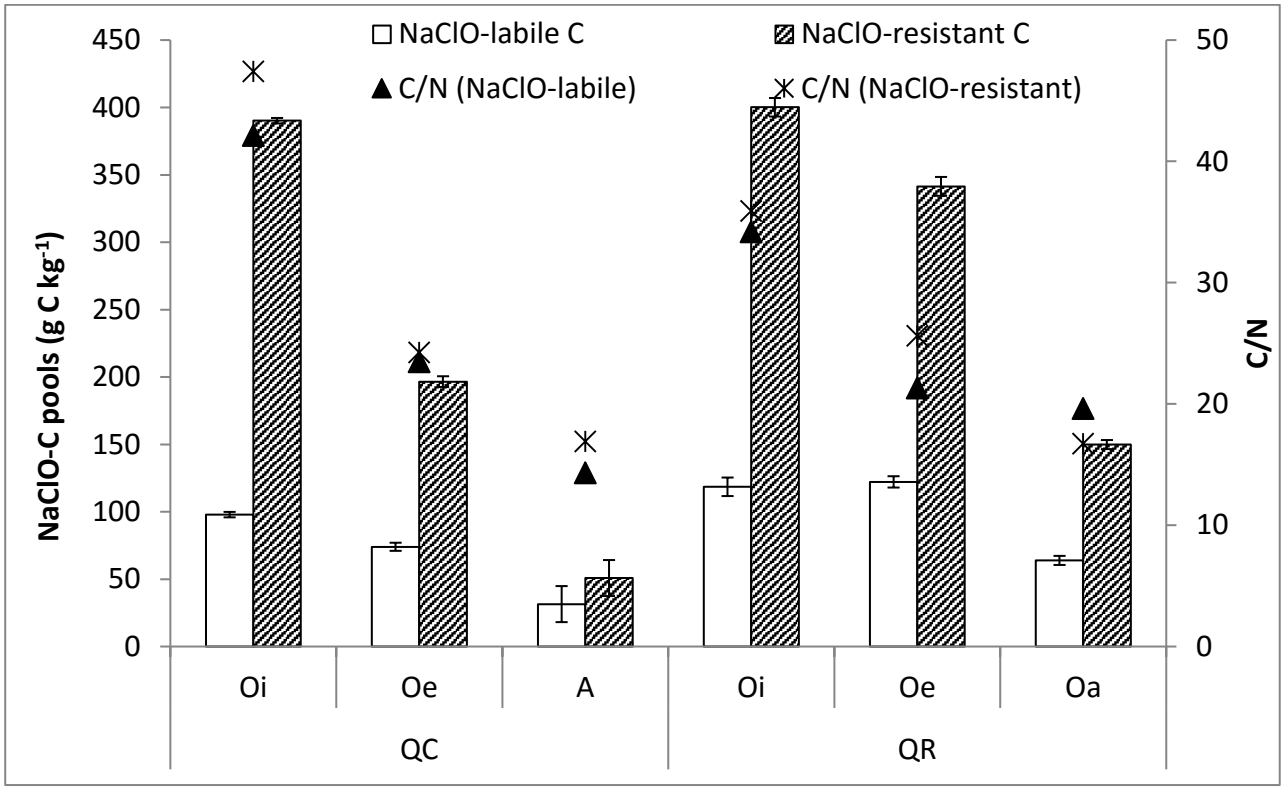
NaClO-labile C
NaClO-resistant C
C/N (NaClO-labile)
C/N (NaClO-resistant)
NaClO-C pools (g C kg-1)
C/N
450
400
350
300
250
200
150
100
50
0
50
40
30
20
10
0
Oi
Oe
A
Oi
Oe
Oa
QC
QR
Figure 4

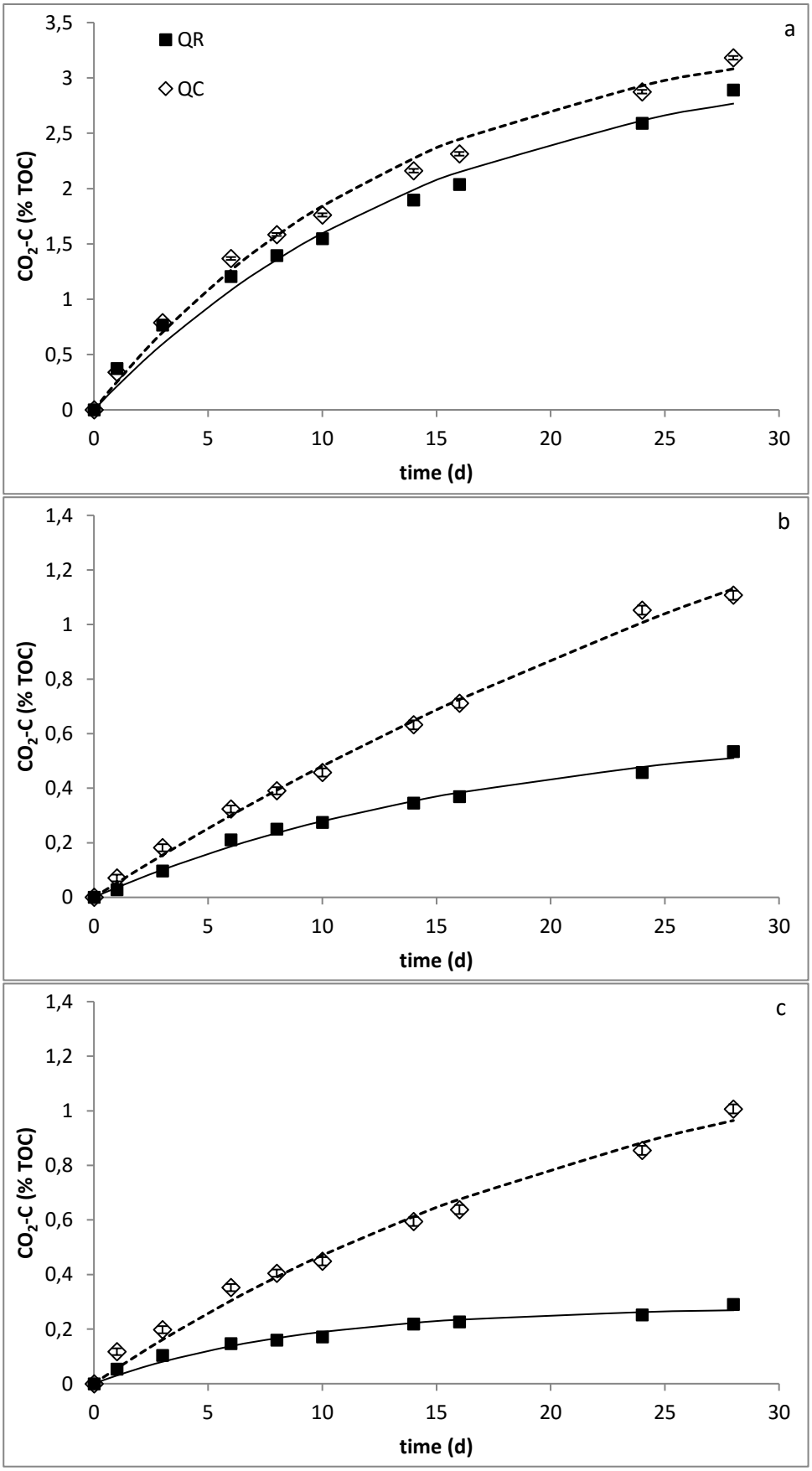

Figure 5

Table 1. Selected properties of the soil samples at the *Quercus robur* L. (QC) and *Quercus rubra* L. plots (QR) in the La Mandria Park. The data are reported as mean (n=5) of the plot and standard deviation (in parentheses)

site	horizon	Upper limit[a]	Lower limit[a]	pH[b]	TOC	TN	TOC/TN	Coarse sand	Fine sand	Coarse silt	Fine silt	Clay	Fe_D[c]	Fe_D/Fe_T
		cm	cm		g kg^{-1}	g kg^{-1}		%	%	%	%	%	g kg^{-1}	
QC	Oi	0	5	5.3	488.8 (10.6)	10.8 (0.9)	48.7							
	Oe	5	6	5.8	275.3 (13.3)	11.5 (1.2)	26.0							
	A	6	9	5.0	83.9 (6.5)	5.4 (0.7)	16.0	1.9 (1.5)	30.8 (2.8)	21.3 (2.8)	28.4 (0.7)	17.5 (1.0)	1.7 (1.0)	0.29
	AE	9	28	4.4	9.3 (0.9)	0.8 (0.1)	11.7	0.5 (0.1)	42.5 (1.4)	13.1 (1.5)	24.9 (0.2)	19.1 (0.6)	12.8 (1.2)	0.30
	E	28	43	4.7	3.8 (0.6)	0.5 (0.1)	6.2	0.5 (0.1)	35.2 (2.4)	19.3 (0.7)	26.5 (0.6)	18.4 (1.7)	13.9 (1.3)	0.32
	Bt1	43	61	5.0	2.5 (0.4)	0.5 (0.1)	4.2	0.4 (0.1)	24.0 (1.3)	22.2 (1.1)	29.3 (1.0)	24.1 (0.4)	16.2 (2.4)	0.36
	Bt2	61	81	5.1	1.9 (0.3)	0.4 (0.1)	3.0	0.3 (0.0)	28.0 (1.9)	20.7 (0.7)	26.7 (0.6)	24.2 (1.0)	16.9 (0.8)	0.37
	Btx	81	100	5.4	1.5 (0.2)	0.4 (0.1)	3.3	0.4 (0.1)	22.1 (4.0)	24.6 (1.6)	27.2 (0.8)	25.7 (2.6)	19.1 (1.2)	0.39
QR	Oi	0	5	5.0	514.2 (14.0)	14.6 (1.2)	38.6							
	Oe	5	6	5.9	463.5 (14.3)	19.3 (1.4)	25.5							
	Oa	6	11	4.3	215.4 (12.1)	12.4 (0.7)	16.6	5.4 (0.8)	53.6 (3.5)	11.8 (4.1)	17.3 (0.8)	11.8 (0.3)	13.1 (0.7)	0.31
	E1	11	36	4.4	11.5 (1.3)	0.9 (0.1)	12.6	0.5 (0.1)	38.2 (2.9)	21.1 (1.4)	24.9 (1.5)	15.4 (0.5)	14.5 (1.2)	0.31
	E2	36	45	4.6	6.7 (0.8)	0.5 (0.1)	12.2	0.4 (0.1)	30.7 (1.5)	24.5 (1.1)	26.7 (0.4)	17.7 (1.7)	15.4 (1.1)	0.34
	Bt	45	56	4.8	3.6 (0.5)	0.4 (0.0)	7.5	0.2 (0.1)	29.0 (4.0)	22.3 (1.1)	24.6 (0.8)	23.8 (2.6)	20.1 (1.2)	0.40
	Btx	56	86	5.3	2.0 (0.3)	0.4 (0.1)	4.0	0.3 (0.0)	24.3 (1.6)	22.8 (1.3)	24.7 (0.9)	27.8 (1.4)	11.7 (1.0)	0.31

[a] upper and lower limits refer to the soil profile
[b] the pH data were obtained on the soil profile only
[c] Fe_D: dithionite-citrate-bicarbonate extractable Fe; Fe_T: total Fe

Table 2. Element availability and total contents of the soil samples at the *Quercus robur* L. (QC) and *Quercus rubra* L. (QR) plots in the La Mandria Park. The data are reported as mean (n=5) of the plot and standard deviation (in parentheses)

		CEC[a]	Ca_{ex}	Mg_{ex}	K_{ex}	Al_{ex}	BS[a]	Ca_T	Mg_T	K_T	P_T	P_{av}
		$cmol_c\ kg^{-1}$	$cmol_c\ kg^{-1}$	$cmol_c\ kg^{-1}$	$cmol_c\ kg^{-1}$	$cmol_c\ kg^{-1}$	%	$g\ kg^{-1}$	$g\ kg^{-1}$	$g\ kg^{-1}$	$mg\ kg^{-1}$	$mg\ kg^{-1}$
QC	Oi							46.2 (2.09)	13.9 (0.39)	12.4 (0.39)	2950 (37)	
	Oe							12.6 (2.69	2.9 (0.19	12.1 (0.19	1460 (23)	
	A	18.3 (1.1)	5.45 (0.05)	1.80 (0.07)	0.32 (0.01)	1.07 (0.06)	41.3	4.6 (0.4)	6.8 (0.2)	9.0 (0.1)	438 (6)	20.2 (0.9)
	AE	8.2 (0.2)	0.23 (0.02)	0.19 (0.00)	0.02 (0.00)	0.63 (0.05)	5.4	4.4 (0.1)	7.4 (0.1)	10.6 (0.4)	208 (9)	1.7 (0.1)
	E	7.0 (0.1)	0.34 (0.03)	0.41 (0.02)	0.02 (0.00)	0.36 (0.03)	11.0	4.5 (0.2)	8.0 (0.2)	11.9 (0.2)	215 (7)	0.9 (0.1)
	Bt1	9.2 (0.2)	1.16 (0.06)	1.66 (0.05)	0.03 (0.01)	0.11 (0.04)	30.9	4.2 (0.1)	8.7 (0.2)	13.9 (0.1)	221 (7)	1.8 (0.0)
	Bt2	9.8 (0.1)	1.81 (0.14)	2.18 (0.02)	0.02 (0.01)	0.05 (0.02)	40.8	4.0 (0.2)	7.7 (0.1)	12.5 (0.1)	234 (6)	2.4 (0.0)
	Btx	9.8 (0.2)	2.17 (0.06)	2.65 (0.11)	0.03 (0.00)	0.05 (0.03)	49.5	3.9 (0.1)	7.8 (0.2)	12.6 (0.1)	256 (8)	3.6 (0.1)
QR	Oi							45.1 (1.1)	19.3 (1.2)	11.6 (0.5)	4121 (47)	
	Oe							37.3 (4.1)	9.8 (0.3)	11.5 (0.1)	2409 (75)	
	Oa	38.5 (5.7)	1.86 (0.23)	0.67 (0.17)	0.66 (0.11)	nd	6.8	5.4 (0.7)	3.1 (0.3)	9.6 (0.2)	1019 (28)	1.9 (1.9)
	E1	6.6 (0.1)	0.18 (0.02)	0.25 (0.03)	0.02 (0.00)	0.48 (0.03)	6.8	4.9 (0.3)	6.9 (0.1)	9.7 (0.1)	159 (8)	1.5 (0.1)
	E2	5.5 (0.1)	0.25 (0.02)	0.57 (0.03)	0.02 (0.00)	0.18 (0.03)	15.1	4.4 (0.4)	7.6 (0.2)	9.0 (0.2)	148 (7)	0.7 (0.1)
	Bt	8.3 (0.2)	0.57 (0.06)	1.63 (0.03)	0.02 (0.01)	0.06 (0.02)	26.9	4.4 (0.1)	7.6 (0.3)	10.4 (0.2)	145 (6)	0.6 (0.0)
	Btx	12.4 (0.7)	2.03 (0.12)	3.84 (0.06)	0.03 (0.00)	0.04 (0.01)	47.4	4.4 (0.2)	7.9 (0.1)	12.2 (0.1)	148 (5)	0.5 (0.0)

[a] CEC: cation exchange capacity; BS: Base saturation of the exchange complex

Table 3. Integration values for the major C-types in the ^{13}C NMR spectra of top horizons (chemical shift range in ppm) of the soil profiles under *Quercus robur* L. (QC) and *Quercus rubra* L. (QR) in the La Mandria Park. Ratios between specific spectral ranges.

Shift region(ppm)	***QC***			***QR***		
	Oi	Oe	A	Oi	Oe	Oa
Alkyl C (0-45ppm)	24	22	26	24	27	32
0-30	11	11	13	11	13	15
30-45	13	11	13	13	14	17
O-alkyl C (45-110 ppm)	64	57	49	62	56	49
45-60	8	9	9	8	9	9
60-90	45	37	29	43	37	30
90-110	11	11	11	11	10	10
Aromatic C (110-160 ppm)	9	14	17	11	12	12
110-140	6	9	11	7	8	8
140-160	3	5	6	4	4	4
C=O C (160-220 ppm)	3	7	8	3	5	7
160-180	3	5	5	3	4	5
180-220	0	2	3	0	1	2
Ratios and indexes						
Aryl C/O alkyl C	0.14	0.25	0.35	0.18	0.21	0.24
Alkyl C/O alkyl C	0.38	0.39	0.53	0.39	0.48	0.65
Aromatic C/aliphatic C	0.38	0.64	0.65	0.46	0.44	0.38

Table 4. Respiration parameters (C_0: C mineralization potential in 28 days; K: rate constant) in the top horizons of the soil profiles under *Quercus robur* L. (QC) and *Quercus rubra* L. (QR) in the La Mandria Park.

		QC	*QR*
Oi			
	C_0 % TOC	3.53	3.27

Oe	$K\ d^{-1}$	0.074	0.073
	R^2	0.993	0.98
Oa/A	C_0 % TOC	2.57	0.638
	$K\ d^{-1}$	0.021	0.058
	R^2	0.996	0.992
	C_0 % TOC	1.44	0.281
	$K\ d^{-1}$	0.040	0.112
	R^2	0.986	0.969

.